Journal of the Korean Physical Society (2025) 87:1054–1067
https://doi.org/10.1007/s40042-025-01377-8

Online ISSN 1976-8524
Print ISSN 0374-4884

RESEARCH - PARTICLES AND NUCLEI

Mechanical behavior of storage ring girders in Korea-4GSR under gravity and vibration loads

Gwang-Wook Hong[1] · Hong-Gi Lee[1] · Gyeongsu Jang[1] · Seungha Shin[1] · Taekyun Ha[1]

Received: 31 January 2025 / Revised: 18 April 2025 / Accepted: 24 April 2025 / Published online: 13 May 2025

Abstract
The Korea 4GSR requires a highly precise arrangement of electromagnets, undulators, vacuum chambers, and monitoring devices. These 4th generation accelerators demand micro-level electron beam control with exceptional precision. Specifically, Korea 4GSR is designed to achieve a narrow beam profile, with a target beam size of sub 4.5 μm. To ensure this precision, developing a stable girder system capable of reliably supporting high-accuracy accelerator components is essential. The girder system must be stable enough to span an extensive circumference of approximately 800 m, accommodate mechanical loads without deformation and respond effectively to dynamic conditions associated with the accelerator's operating energy of 4 GeV. Furthermore, the system should mitigate ground irregularities and ensure assembly stability during installation. This study aims to contribute to the stable beam operation of Korea 4GSR by developing a system capable of displacement control and vibration suppression within 10% of the beam size, a mechanical stability target required for next-generation synchrotron radiation facilities, based on a girder system with ensured stiffness.

Keywords 4GSR · Accelerator · Static analysis · Vibration analysis · Mechanical stability

1 Introduction

The performance of synchrotron radiation from next-generation accelerators critically depends on beam stability, in addition to traditional accelerator design goals. Synchrotron users require stable radiation characteristics such as intensity, position, polarization, and coherence to ensure reliable experimental results. Maintaining these constant conditions, collectively known as "beam stability," demands coordinated efforts across all accelerator subsystems. Beam stability is influenced by numerous factors, including accelerator and beamline equipment, infrastructure systems (cooling water, electrical power), mechanical vibrations, temperature variations, electrical noise, and ground movements. Deviations from ideal conditions result in errors, classified as static or dynamic, random or systematic.

Next-generation synchrotron accelerators, such as the ongoing Korea 4GSR (4th Generation Synchrotron Radiation) facility project, exhibit significantly smaller electron beam sizes approximately 10% of those in existing third-generation synchrotrons necessitating more stringent beam stability criteria. Beam stability can be categorized into static and dynamic stability. Dynamic stability further divides into short-term stability (frequency range of 0.1–1 kHz), limiting rapid beam fluctuations within 10% of beam size [1], and long-term stability, maintaining beam position drift below 1 μm over weeks of operation. Static stability pertains to manufacturing precision and alignment accuracy during construction, commissioning, and periodic realignment processes. Precise electromagnet alignment within tens of micrometers is essential to minimize multipole field effects.

A robust girder system significantly reduces beam instabilities caused by mechanical vibrations and ground movements. The girder system for the Korea 4GSR project, currently under construction with an 800 m circumference, is informed by operational experiences from the PLS-II facility. Various girder alignment mechanisms including motor-driven cam movers, manual wedge jacks, and motor-driven wedge jacks are employed worldwide in Table 1 [2–11]. The PLS-II system currently employs screw jack alignment mechanisms providing wide adjustability and structural rigidity. The Korea 4GSR girder system advances this by integrating precision ball screw jacks, offering enhanced

✉ Taekyun Ha
hatae@postech.ac.kr

[1] Pohang Accelerator Laboratory (PAL), POSTECH, Pohang 37673, South Korea

Table 1 Adjustment method of magnet girder and supports for each photon source [2–11]

Facility	Adjustment method	
Spring-8	Manual adjustment	6-Point Support
SOLEIL		4-Wedge jack
SSRF		3-Wedge jacks, 3-Assistant supports
NSLS-II		8-Point support
APS-U		3-Point support, 3-points adjustment
SIRIUS		4-Point wedge jacks
SLS	Automatic adjustment	5-cam mover mechanisms
Diamond		5-cam mover mechanisms
TPS		6-cam mover mechanisms
ESRF-EBS		4-Motorized wedges, 3-Manual sedges

positioning accuracy and durability compared to traditional TM screw jacks. Moreover, it incorporates motor-driven alignment controls and displacement sensors (LVDTs) for precise real-time adjustments during installation and operation.

This study employs numerical analyses using finite element modeling (FEM) to evaluate structural deformation under self-weight loading, identify natural frequencies through modal vibration analysis, and assess dynamic response through random vibration analysis. These analyses optimize the mechanical performance of the proposed girder system for the Korea 4GSR project prior to fabrication.

2 System design

2.1 Girder system requirements for the Korea 4GSR

The girder system for the Korea 4GSR facility must fulfill specific technical requirements distinct from conventional circular synchrotron accelerators. Unlike other upgrade projects transitioning from third- to fourth-generation synchrotrons, primarily using existing infrastructure, the Korea 4GSR project demands a girder system optimized explicitly for new construction and unique ground conditions. The following key criteria must be satisfied:

• **Electron beam height**: maintain the electron beam precisely at 1.4 m above the floor, aligning with beamline standards.

• **Girder surface flatness and minimal deformation**: ensure high flatness and minimal deformation under operational loads. The minimum beam size of Korea 4GSR is approximately 4.5 μm in the x-direction and 2.9 μm in the y-direction. Mechanical stability is a critical consideration for the next-generation synchrotron radiation facility, requiring assurance of mechanical stability within 10% of the Korea 4GSR beam size.

• **High first-order resonance frequency**: achieve high resonance frequencies to effectively minimize vibrations.

• **Motorized precision alignment mechanism**: allow precise positional adjustments for initial installation and periodic realignment.

• **Space-optimized design**: optimize girder geometry to maximize space utilization in the storage ring tunnel for accessibility and maintenance.

• **Mounting interfaces for diverse equipment**: provide strategically positioned mounting holes to accommodate various accelerator components.

• **Enhanced thermal stability**: minimize thermal deformation to maintain component alignment accuracy under varying environmental conditions.

The detailed parameters for the girder system design, including alignment adjustment ranges, resonance frequency targets, adjustment mechanisms, and alignment accuracies, are presented in Table 2.

2.2 Storage ring girder system layout

The Korea 4GSR storage ring, with an 800-m circumference, comprises 28 cells classified into normal cells and High Beta Injection (HBI) cells. Each cell consists of five girders, as illustrated in Fig. 1. The normal cells are symmetrically arranged upstream and downstream relative to the central bending section, with three central girders measuring 4800 mm and two end girders measuring 3800 mm in Fig. 2. HBI cells similarly include three 4800-mm girders centrally, complemented by one 3400-mm girder at the injection section and one 3800-mm girder connecting to a standard cell. All girders feature four-point vertical supports, enabling horizontal and longitudinal beam direction adjustments, providing flexibility and precision in aligning accelerator components.

2.3 Structural design and consideration

The girder system design for the Korea 4GSR facility was carefully developed considering critical requirements such as beam stability, precise alignment, mechanical rigidity, and ease of installation and maintenance. As illustrated in Fig. 3, the girder system primarily consists of three main components: the girder body, vertical support structures, and adjustment mechanisms. The vertical support structures are engineered to withstand a total load capacity of 15 tons, comprising the self-weight of the girder body (approximately 5 tons) and the additional weight of accelerator components, including electromagnets, vacuum chambers, and diagnostic equipment (approximately 10 tons).

Table 2 Key parameter for the girder system

Parameter	Value			
	Korea 4GSR	ESRF-EBS	APS-U	HEPS
# of Cell	28 cells	32 cells	40 cells	48 cells
Circumference or SR	798.8 m	844 m	1100 m	1360.4 m
Beam height	1.4 m	1.2 m	1.4 m	1.2 m
Leveling range (Y-axis)	±10 mm	±5 mm	±13 mm	±9 mm
Lowest natural frequency (Girder only)	50 Hz	50 Hz	42 Hz	54 Hz
Maximum Girder length	<5 m	5.1 m	5.568 m	3.8 m
Girder to girder alignment	±50 μm	50 μm	50 μm rms	±50 μm
Adjustment method (Y-axis)	Motorized	Motorized	Manual	Manual
Adjustment method (X, Z-axis)	Manual	Manual	Manual	Manual
Positioning accuracy (Y, X-axis)	±50 μm	50 μm	30 μm	±50 μm
Positioning accuracy (Z-axis)	±200 μm	1 mm	70 μm	±200 μm

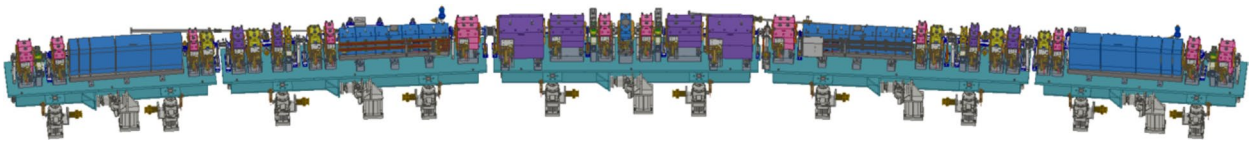

Fig. 1 Design of the girder in the achromat

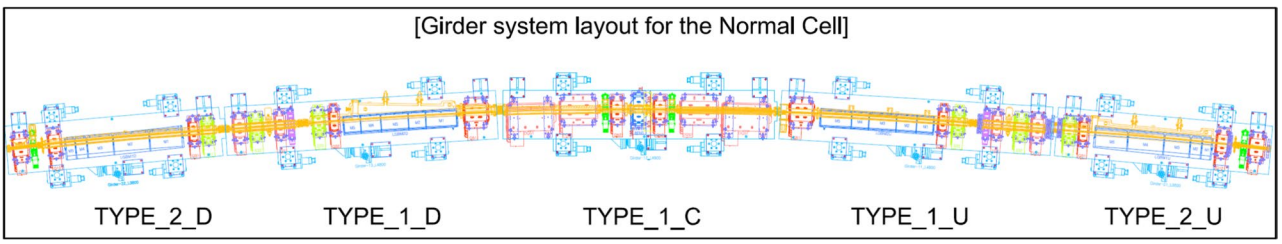

Fig. 2 Girder system layout in the storage ring

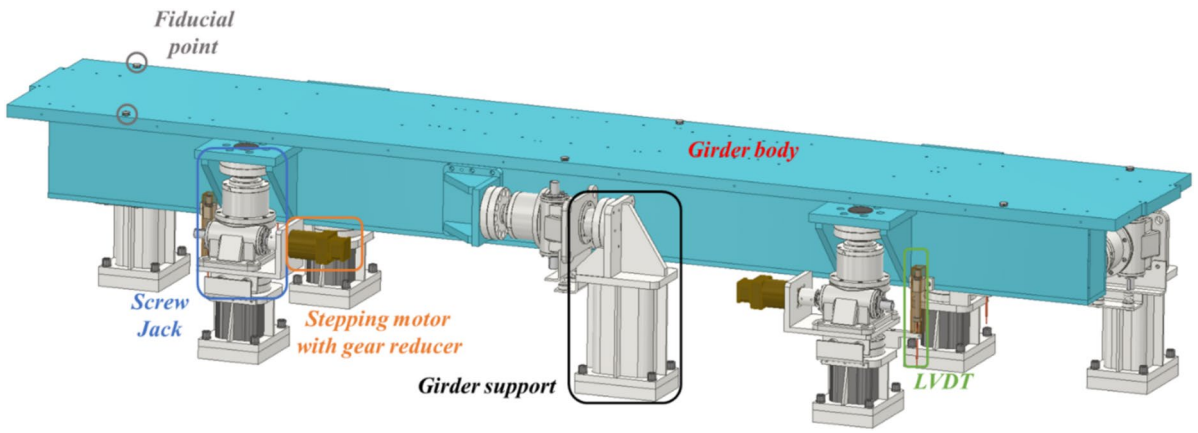

Fig. 3 Girder design

Table 3 Specification of girder system

Parameter		Type 1	Type 2	Type 3
Girder body	Quantity of Girder [set]	84	52	4
	Total length [m]	4.8	3.8	3.4
Adjustment System	Vertical adjusting method	Stepping Motor with Screw Jack		
	Transverse and longitudinal adjusting method	Manual with Screw jack		
	Quantity of screw jack [set]	588	364	28
	Quantity of stepping motor system [set]	336	208	16
	Quantity of LVDT [set]	336	208	16
	Max. torque for the stepping motor [N*m]	3.88		
	Loading capacity of screw jack [ton]	12		
	Feed rate per revolution of screw jack [mm]	1.25		
	Gear ratio of gear reducer [ratio]	320:1		
	Feed rate per revolution after gear [μm]	3.9		
	Working range of screw jack [mm]	±20 (40)		
	Measure range of LVDT [mm]	±10 (20)		

Table 4 Mechanical properties of the girder material

Mechanical Properties	Value	
	SS400	S45C
Density	7.85e-6 [kg/mm3]	7.85e-6 [kg/mm3]
Tensile strength	415–515 [MPa]	686 [MPa]
Young's Modulus	160 [GPa]	205 [GPa]

The detailed specifications of the storage ring girder design are summarized in Table 3. This includes the quantity of each type of girder, performance characteristics of the adjustment mechanisms, and specific parameters of the girder monitoring system. To achieve the required mechanical rigidity, stability, and ease of fabrication, the girder components are planned to be manufactured using structural steels SS400 and S45C, chosen for their optimal balance between mechanical strength, rigidity, and machinability. Mechanical properties of these selected materials are presented in Table 4.

The girder adjustment system incorporates seven adjustment devices arranged to allow positional adjustments in vertical, horizontal, and longitudinal directions, as illustrated in Fig. 4. Vertical adjustments, primarily bearing operational loads, utilize a motor-driven system employing precision ball screw jacks for accurate and convenient alignment during installation and maintenance. Adjustments in the horizontal and beam lattice directions are manually operated to accommodate critical initial alignment procedures and beam operations.

To achieve the required stiffness and load-bearing capability, structural reinforcements including internal ribs and additional reinforcing bars are strategically placed within the girder body, at the girder top surface, and at attachment points for adjustment devices. Table 5 outlines the load capacities, demonstrating vertical supports designed for loads exceeding 7 tons per point, totaling over 20 tons. Horizontal and longitudinal adjustments can support more than 450 kg and 900 kg, respectively, ensuring the required robustness and rigidity for stable accelerator operation.

Table 5 Load distribution applied to the adjustment device

Screw Jack	Static load [kgf]	Seismic Load [kgf]	Total Load [kgf]
V1	3691	3928	7619
V2	3670	3904	7574
V3	3620	3844	7464
V4	3612	3835	7447
H1	0	460	460
H2	0	458	458
L1	0	918	918

To enhance dynamic characteristics, such as increasing the natural frequency of the girder system, the structural design aimed to maximize rigidity while minimizing total weight. To achieve an optimal stiffness to weight ratio for the Korea 4GSR girder system, the girder height was limited to 600 mm, and the plate thickness was standardized at approximately 20 mm. Additionally, the internal reinforcements were strategically shape optimized to minimize overall weight while ensuring sufficient resistance against gravitational deformation and torsional stresses.

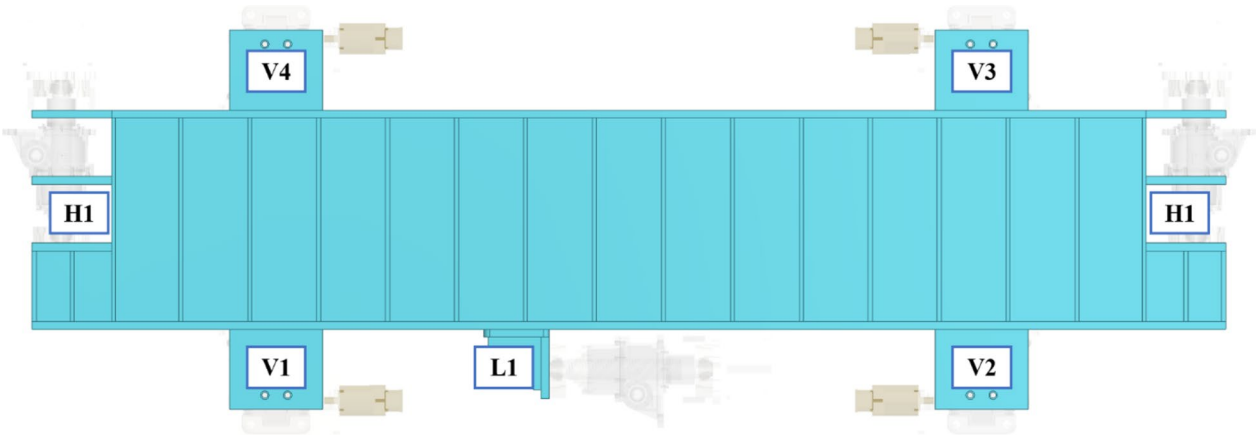

Fig. 4 Structural reinforcement and Load point of the girder body

$$f_n = \frac{1}{2\pi}\sqrt{\frac{k}{m}}$$

f_n : Natural frequency

k : Stiffness of the system

m : Effective mass

The adjustment mechanism of the girder system is illustrated in Fig. 5. It consists of seven adjustment devices allowing positional adjustments in vertical, horizontal, and longitudinal directions. The vertical adjustment system, primarily bearing operational loads, employs a motor driven ball screw jack for precise and convenient alignment during

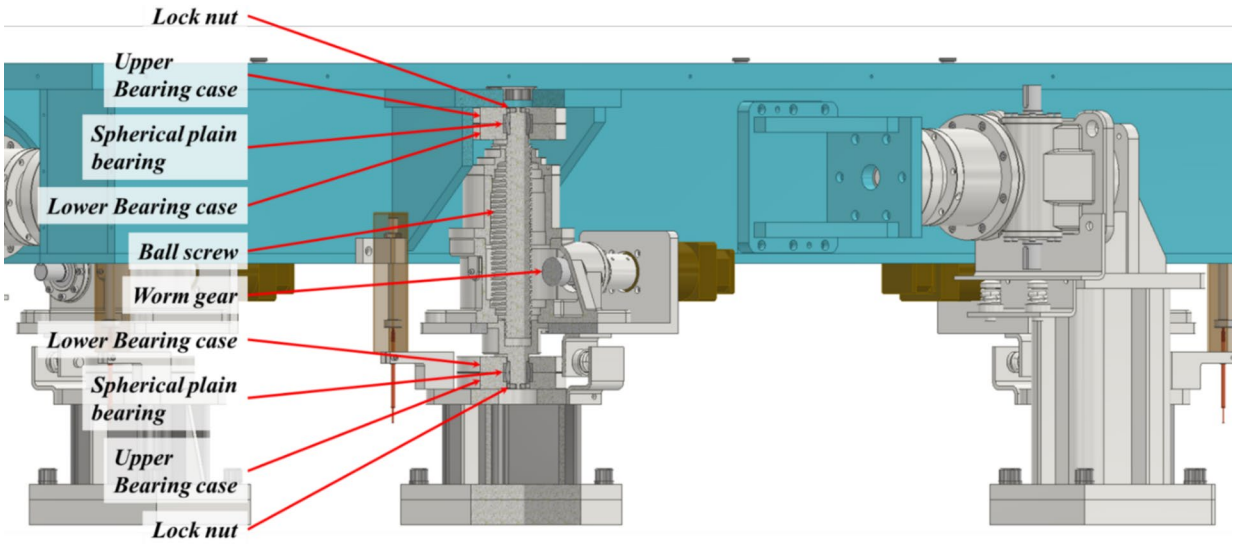

Fig. 5 Assembly of ball screw jack and girder support

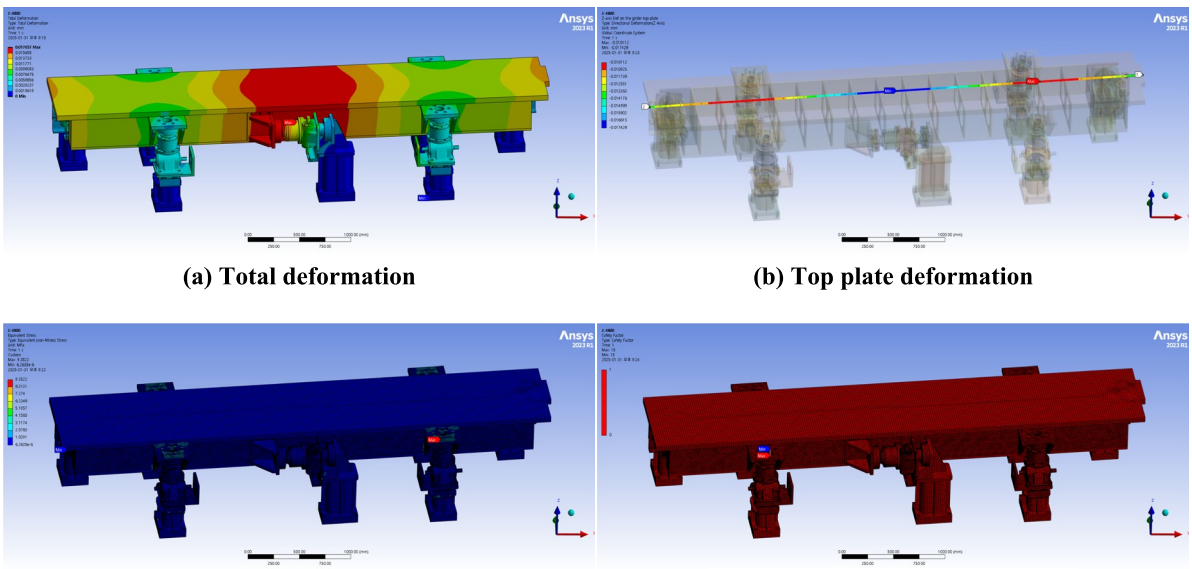

Fig. 6 Result of static analysis

Springer KPS 한국물리학회 The Korean Physical Society

Table 6 Displacement comparison by weight and type of girders

Type of girder	Displacement [μm]		Shape of result	Note
	Total	Top plate of girder (Dev. of flatness)		
Type_1	17.4	7.42	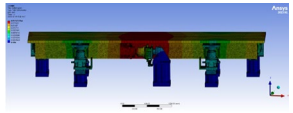	Own weight (4.5 ton)
	49.1	14.44	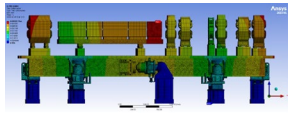	Type_1_U (9.6 ton)
	75.6	21.84	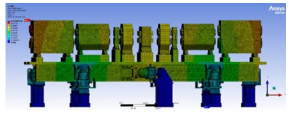	Type_1_C (13.5 ton)
Type_2	12	3.77	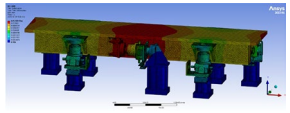	Own weight (3.9 ton)
	44	6.22	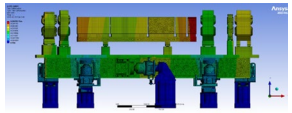	Type_2_U (7.8 ton)

installation and maintenance. A high-precision alignment of approximately 4 μm was achieved through the utilization of ball screw jacks coupled with a high gear ratio mechanism. Adjustment devices in horizontal and longitudinal directions utilize manual methods, providing positional adjustments critical for initial alignment and operation.

The ball screw based vertical adjustment devices are assembled using disk shaped bearing cases connecting the girder body and adjustment units. These bearings include spherical plain bearings positioned between the bearing disks, allowing rotation when the fastening torque is loosened, facilitating ease of installation and maintenance. Increasing the fastening torque fixes the angular position, enhancing mechanical rigidity of the assembly.

The adjustment devices are located strategically at both ends of the girder body and lower supports, ensuring sufficient margin for precise installation and maintenance. Considering structural rigidity, the lower casing of the adjustment device was reinforced by optimizing its thickness and reducing its length, effectively increasing mechanical stiffness without adding unnecessary structural complexity. High strength steel S45C, known for superior mechanical rigidity compared to conventional carbon steel, was selected for ball screw jack components. The vertical adjustment motions within confined spaces are achieved using a step motor coupled with a worm gear, converting rotational motion into linear vertical displacement. The ball screw jack features dual safety mechanisms: a mechanical stopper on the worm ear shaft and an integrated motor braking function, providing robust protection against unintended displacement.

Furthermore, high-precision displacement measurement is realized using linear variable displacement transducer (LVDT) sensors. The displacement data obtained from the LVDT sensors are continuously monitored by the control system, enabling precise motor driven adjustments and real time position monitoring during accelerator operation.

3 Analysis of stiffness and frequency responsiveness

3.1 Static structural analysis

Static structural analysis was conducted using finite element analysis (FEA) to evaluate deformation and stress distribution due to gravitational loading on the girder system. The initial analysis focused on the stiffness assessment of the girder system itself. The analysis encompassed the entire girder assembly, including the girder body and associated adjustment mechanisms, using ANSYS software. A representative girder model with a length of 4800 mm in the longitudinal direction was selected for this analysis, as it represents a critical load-bearing configuration.

As depicted in Fig. 6, the maximum vertical displacement caused by gravitational loading (self-weight) was determined to be 17.4 μm. This peak deformation occurs at the mid-point along the girder length, corresponding closely to the girder's center of gravity. The displacement variation of the girder top plate was observed to be 7.42 μm. Furthermore, the maximum von Mises stress within the girder system was calculated to be 9.35 MPa, predominantly concentrated at the interfaces between the girder body and the vertical adjustment mechanisms, reflecting the localized load transmission through the vertical supports. A structural safety factor evaluation indicated a safety factor of approximately 15, demonstrating robust structural integrity under operational loading conditions.

Table 6 summarizes the displacement analysis results for different girder configurations, including scenarios where the girder supports electromagnets of varying weights. The analysis utilized a simplified electromagnet model that accounts for mass distribution and center of gravity positioning, facilitating computational efficiency without compromising result accuracy. Consistently, maximum deformation occurs centrally on the girder top surface, diminishing progressively toward the girder supports. These displacement patterns affirm that the girder design achieves a stable structural response within the acceptable tolerance range, supporting precise accelerator component alignment and maintaining beam stability requirements.

The static analysis results showed that Type 2, the lightest girder configuration, exhibited a maximum deflection of 12 μm, whereas Type 1 with CBM, the heaviest configuration, exhibited a deflection of 75.6 μm. The influence of errors on the beam has already been investigated [12]. The study analyzed the effects of various errors, including girder errors, on the beam. However, it is inherently challenging to isolate and evaluate the impact of girder errors exclusively from the cumulative effects of all errors. Moreover, examining the influence on beams by considering only girder errors is impractical. Consequently, the influence of

Table 7 Storage ring magnet and girder tolerance (rms value)

Magnet	Misalignment [μm] (X/Y/Z)	Rotation [μrad] (Roll/Pitch/Yaw)	Strength error (%)
LGBM	30/30/250	400/100/100	0.05
Combined-function magnet	30/30/250	400/100/100	0.05
Quadrupole	30/30/250	400/700/700	0.05
Center bend	30/30/250	400/100/100	0.05
Sextupole	30/30/250	400/700/700	0.05
Octupole	30/30/250	400/700/700	0.05
Girder	100/100/100	400/–/–	–

our girder design on beams can only be inferred indirectly by comparing it with results from previous studies.

In prior research, a girder error of approximately 100 μm resulted in an orbit distortion of 110 μm and a reduction in dynamic aperture from 11 to 7 mm. In contrast, the anticipated girder displacement error following the current girder design is expected to be less than 100 μm, suggesting that its impact on the beam will similarly be reduced.

Table 7 summarizes the misalignment, rotation, and strength errors utilized in the previous study. The errors for each element were randomly generated following a Gaussian distribution with 2σ cut-off, meaning any error exceeding 2σ was regenerated to remain within this threshold. The values in the table represent the standard deviation of the errors. Consequently, the girder misalignment error can be ± 200 μm which is an overestimated value compared to the expected displacement error in our girder design. On top of the girder misalignment error, additional element misalignment errors are incorporated, as depicted in Fig. 7.

In addition to misalignment errors, the rotation errors and strength errors were integrated into the analysis, generating 50 error ensembles to assess their collective impact on the beam. Figure 8 illustrates the cumulative distribution function of rms orbit throughout the entire ring. The blue line corresponds to the horizontal rms orbit distortion, while the red line corresponds to the vertical rms orbit distortion. Among 50 ensembles, 80% exhibit a horizontal orbit distortion smaller than 104 μm, and a vertical orbit distortion smaller than 117 μm.

Using the 50 ensembles, the dynamic aperture was also estimated and is presented in Fig. 9. In the ideal case, the dynamic aperture ranges from – 11 to 12 mm. However, the inclusion of errors leads to a reduction in the dynamic aperture. Each ensemble is represented by dots and the mean value is indicated by the orange line. The mean dynamic aperture is approximately 8 mm and even in the worst case, it remains larger than 6 mm.

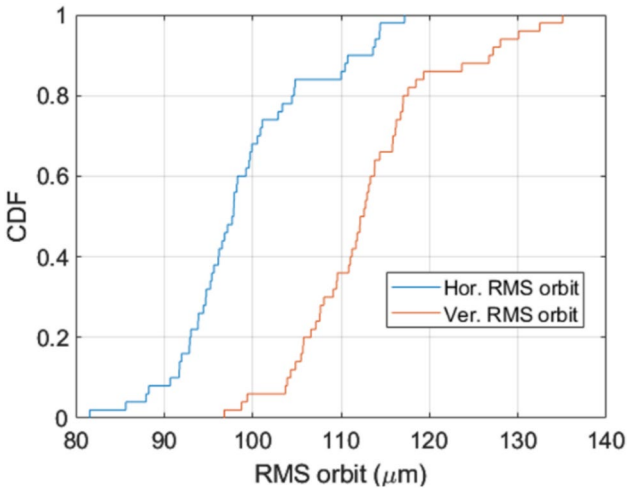

Fig. 8 Cumulative distribution function of RMS orbit after correction

3.2 Modal analysis

Considering the structural and material properties of the girder system, modal analysis based on linear vibration theory and finite element method (FEM) [13] was performed to optimize dynamic characteristics, specifically aiming to increase the system's natural frequencies. As structural resonance can adversely affect beam stability and accelerator operation, achieving sufficiently high natural frequencies is essential.

The modal analysis results presented in Fig. 10 and Table 8 indicate that the first natural frequency of the Type_1 girder system was calculated to be approximately 53.28 Hz. however, further design optimization may be necessary to ensure adequate vibration isolation and minimal excitation under operational conditions.

Modal analysis confirmed the first natural frequency of the girder system to be above the required 50 Hz. In

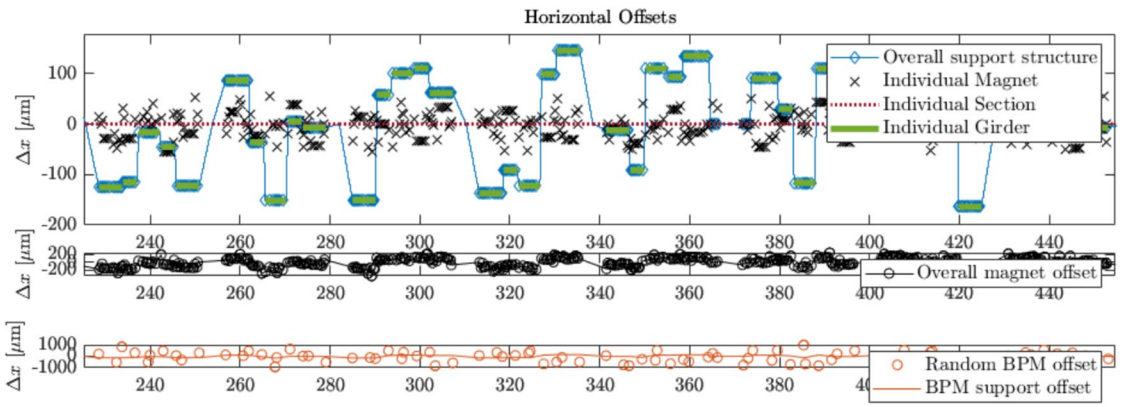

Fig. 7 Horizontal magnet offset along longitudinal position for an arbitrary random error seed

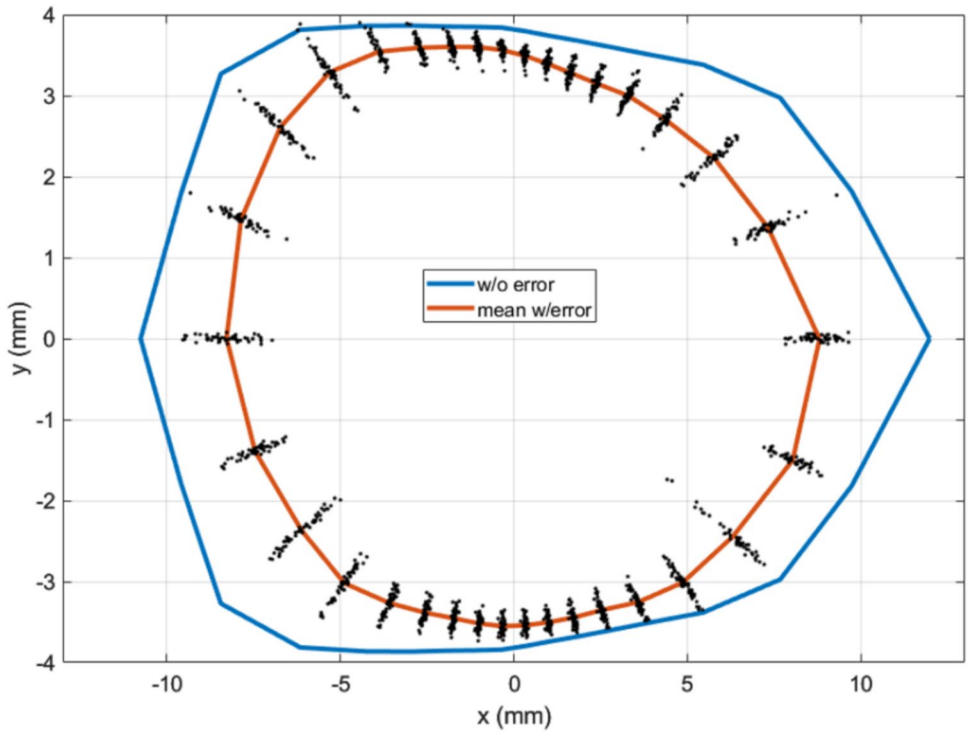

Fig. 9 Dynamic aperture of the lattice ensemble after correction

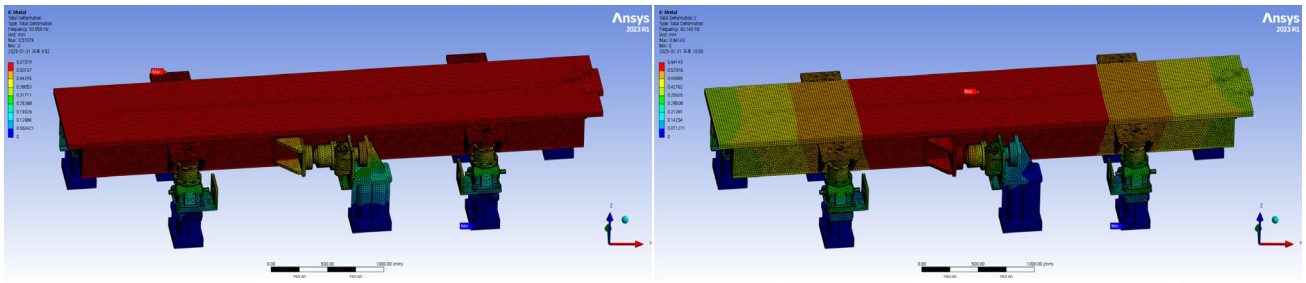

(a) 1st mode (b) 2nd mode

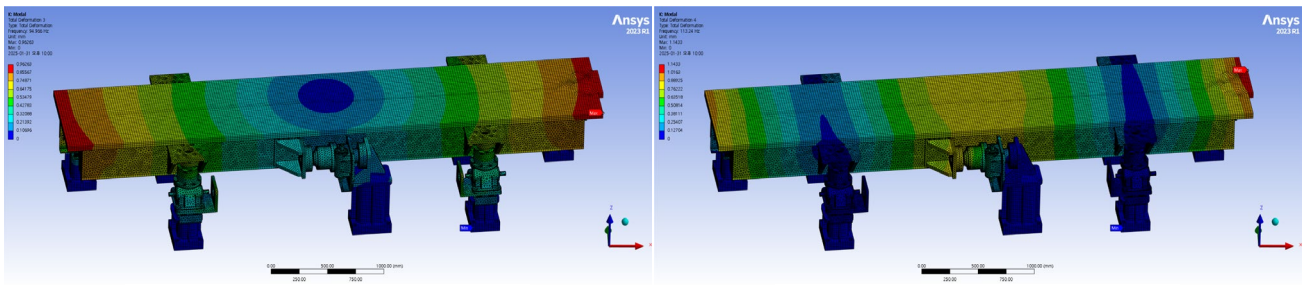

(c) 3rd mode (d) 4th mode

Fig. 10 Result of modal analysis

Table 8 Result of natural frequency with mode and mechanical properties for the Type_1

Mode	Frequency [Hz]	Type
1st	53.286	Transversal translation
2nd	62.949	Transversal translation + Roll
3rd	94.912	Torsional
4th	110.3	Vertically moving motion

this analysis, natural frequency analysis was conducted for the first to fourth modes. The first and second modes exhibited girder motions similar to the beam propagation direction. Furthermore, the third mode showed girder movement in the horizontal direction relative to the beam, while the fourth mode displayed girder movement perpendicular to the beam propagation direction. Although the fourth mode's frequency exceeds 100 Hz, a more precise analysis will be performed on the actual fabricated system, considering the vertical movement of the girder. As the current system excludes the influence of surrounding equipment, the impact of power supplies and cooling systems on the girder will be evaluated through further research.

3.3 Random vibration analysis

Ensuring mechanical stability is crucial for maintaining reliable accelerator operation and beam quality. The mechanical stability in synchrotron accelerators involves effectively mitigating vibrations originating from various external sources, including environmental conditions, external vehicle traffic, mechanical impacts, and vibrations from internal facility systems. Among these sources, natural ground vibrations resulting from geological characteristics, seasonal variations, and seismic events directly propagate through the facility's structure, impacting accelerator components.

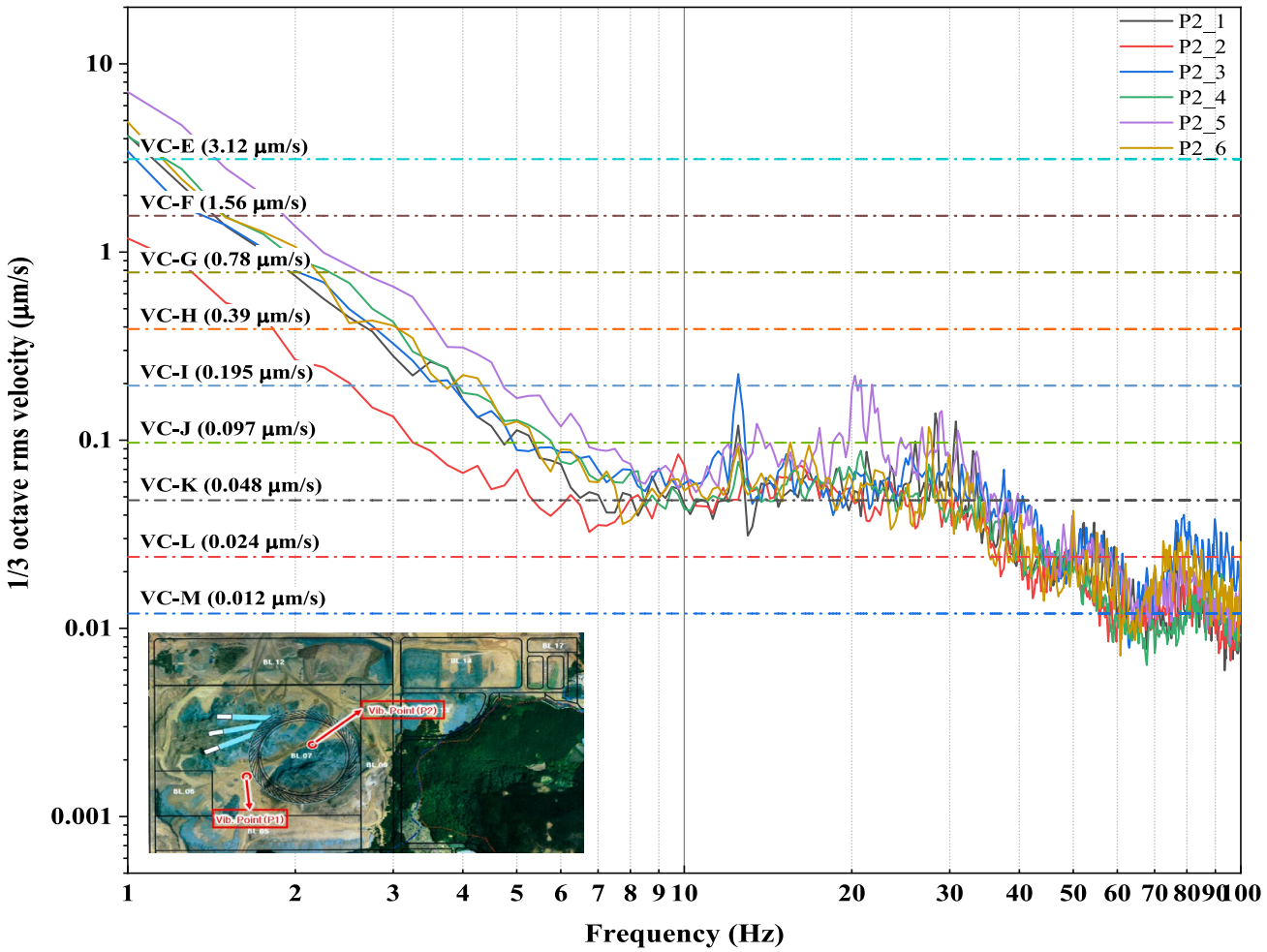

Fig. 11 Ground vibration value on the Korea 4GSR

Table 9 Random vibration data for the girder system

Contents		Value	Note
Deformation [mm]	Total	4.06×10^{-7}	Vertical axis
	Top plate	3.97×10^{-7}	Vertical axis
Stress [MPa]	1-Sigma	1.52×10^{-4}	Probability: 68.269%
	2-Sigma	3.04×10^{-4}	Probability: 95.45%
	3-Sigma	4.56×10^{-4}	Probability: 99.73%
PSD response with natural Freq [μm^2/Hz]	1st mode	1.56×10^{-17}	at 53.859 Hz
	2nd mode	3.13×10^{-18}	at 63.143 Hz
	3rd mode	2.79×10^{-19}	at 94.966 Hz

Therefore, it is imperative to measure and analyze site specific ground vibration characteristics to ensure accelerator stability.

Since the girder system is the primary structure transmitting ground vibrations to the accelerator components, it requires targeted vibration suppression strategies based on accurate ground vibration data. To achieve this, the vibration measurements were performed using an accelerometer with a sensitivity of 10 V/g. Figure 11 shows ground vibration data measured at the Korea 4GSR accelerator construction site. Utilizing this measured ground vibration data, a random vibration analysis was conducted to evaluate the dynamic response and structural stability of the girder system under realistic operational conditions.

Modal analysis provides important natural frequency data; however, it does not directly quantify structural displacement under realistic external excitation conditions due to its inherent analytical limitations. Therefore, random vibration analysis was conducted to accurately predict the girder system's displacement response based on actual ground vibration measurements. Table 9 summarizes displacement results from random vibration analysis, indicating a very small vertical displacement of 39.7 pm at the top surface of the girder. Additionally, PSD (power spectral density) response values corresponding to the girder's natural frequencies were measured at approximately 1.56×10^{-17}, 3.13×10^{-18}, and 2.79×10^{-19} μm2/Hz for the first to third modes, respectively. These displacement magnitudes are negligible compared to the electron beam size requirements of the Korea 4GSR, verifying the excellent mechanical stability and suitability of the proposed girder design.

Figure 12 presents the PSD responses obtained from random vibration analysis for different measurement positions, including the girder support base, support mid-plane, girder top surface, and magnet top surface. It clearly demonstrates vibration amplification at frequencies slightly offset from natural frequencies identified in modal analysis. Furthermore, a progressive increase in vibration amplitude was observed from the girder support base toward the magnet surface, highlighting the importance of structural damping and vibration isolation for achieving the necessary beam stability.

$$\left\langle \frac{y_{co}^2(s)}{\beta_y(s)} \right\rangle = \frac{\langle \Delta Y^2 \rangle}{8\sin^2 \pi \nu_y} \sum_{\text{quads}} \beta_y (k_1 L)^2$$

Data acquired through random vibration analysis can be utilized as fundamental information for assessing beam stability. PSD data transferred to girders and magnets via ground vibrations can be converted into displacement. Particularly, positional stability in quadrupole magnets is an amplification factor. Based on the data in Fig. 12 and the analyzed data, the integrated displacement value of the

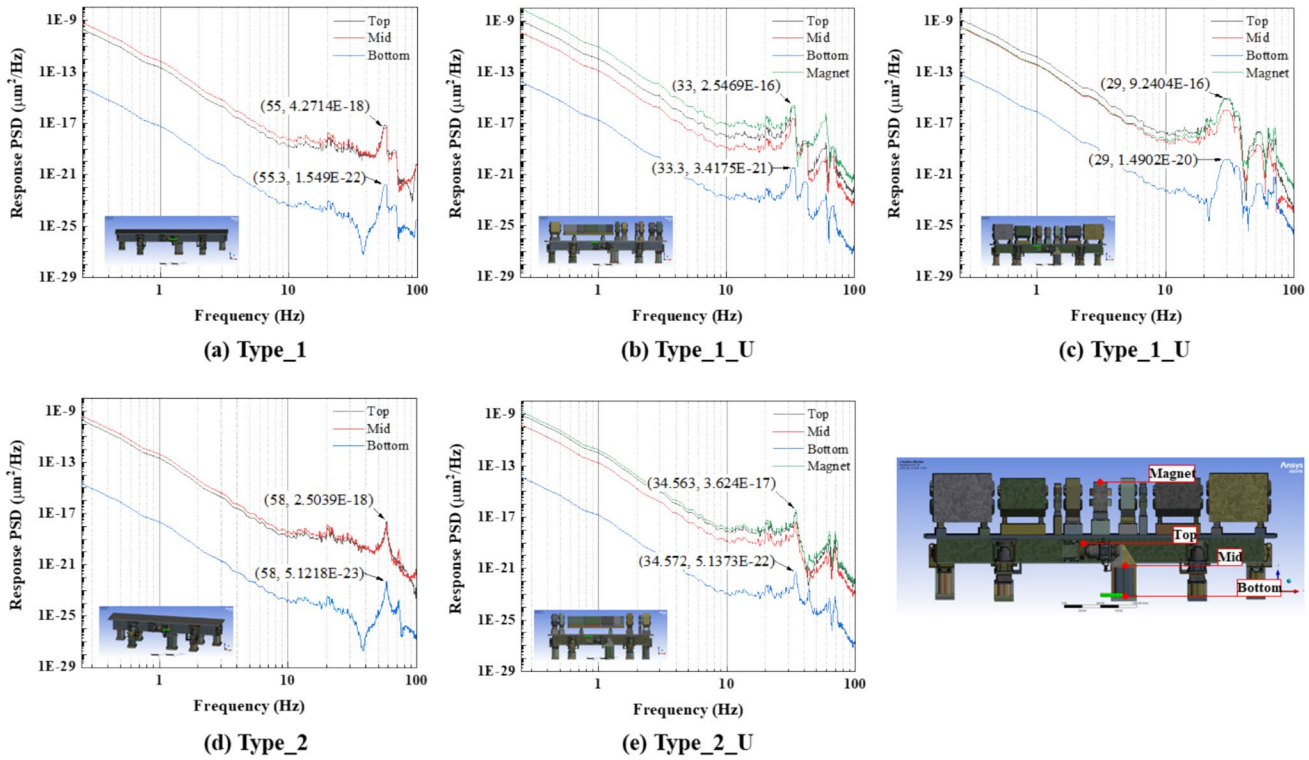

Fig. 12 Response for the PSD and Value position

quadrupole magnet was evaluated to be 80 nm, which is approximately 2% of the beam size. The above equations can be employed to analyze random alignment errors. Assuming a random alignment of the quadrupole magnets, the equations were applied. Upon calculating the random errors for the quadrupole electromagnets on each girder using these equations, the total distortion in the Y-direction was determined to be 21 times the initial value. Substituting this into the electromagnet displacement, the actual displacement error was confirmed to be approximately 1.85 μm.

4 Conclusion

This study presents a comprehensive analysis of the basic design, mechanical stability, and beam stability of the girder system designed for the Korean 4GSR. The basic design of the girder system focuses on providing stable support and enabling precise motion of the electromagnets and vacuum components positioned according to the beam orbit based on beam physics. The mechanical stability of the girder system was assessed using finite element analysis, which included static analysis under gravitational loading and dynamic analysis of frequency characteristics.

From a structural perspective, static analysis confirmed that both the girder assembly and the post-installation displacement of the electromagnets remain well within the allowable tolerance limits. Additionally, the safety factors of the materials employed were found to be considerably high, indicating robust mechanical stability.

When the structural simulation results were compared with beam dynamics analyses, it was evident that the current girder design maintains beam stability within acceptable thresholds. The reduced displacement errors contribute to minimizing orbit distortion and support the preservation of dynamic aperture. These findings collectively confirm that the proposed girder structure effectively satisfies both mechanical and beam physics requirements.

In the dynamic analysis, the natural frequency of the girder system was found to exceed the target value of 50 Hz, and the motion characteristics of the girder system were analyzed for each mode. Random frequency analysis showed that the displacement of the electromagnet due to ground vibrations was at the level of 39.7 pm, and the integrated

displacement in the PSD response evaluation was approximately 80 nm.

However, when applied to the actual beam orbit, higher displacement than the target value was observed. This displacement is expected to be sufficiently compensated for by active orbit correction techniques, such as fast orbit feedback (FOFB) and slow orbit feedback (SOFB) systems.

The characteristics of the girder system presented in this study are expected to serve as valuable foundational data for ensuring beam stability. Future plans include the fabrication of a prototype and on-site experiments to validate and improve the findings of this study.

Acknowledgements This research was supported in part by National R&D Program through the National Research Foundation of Korea(NRF) funded by Ministry of Science and ICT(RS-2024-00431718) and supported by the Korean Government(MSIT: Ministry of Science and ICT) (No. RS-2022-00155836, Multipurpose Synchrotron Radiation Construction Project) and also supported by Pohang Accelerator Laboratory (PAL). PAL is supported by Korean Government(MSIT) and POSTECH.

Author contributions Gwang-Wook Hong: Conceptualization (lead); Formal analysis (lead); Methodology (lead); Visualization (equal); Writing – original draft (lead); Writing – review & editing (equal). Hong-Gi Lee: Conceptualization (equal); Visualization (equal). Gyeongsu Jang: Formal analysis (equal); Methodology (equal); Visualization (equal); Writing – original draft (equal). Seungha Shin: Conceptualization (supporting); Visualization (supporting). Taekyun Ha: Conceptualization (lead); Formal analysis (lead); Methodology (lead); Project administration (lead); Writing – review & editing (lead).

Funding This work was supported by the Ministry of Science and ICT (MSIT), South Korea, under grant numbers RS-2022-00155836 and RS-2024-00431718.

Data availability The data that support the findings of this study are available from the corresponding author upon reasonable request.

Declarations

Conflict of interest The authors declare no competing interests.

References

1. C.-H. Huang et al., J. Instrum. **14**, 01 (2019)
2. K. Fukami, et al., 10th Int. Particle Accelerator Conf. (IPAC'19). JACOW Publishing (2019)
3. J. da Silva Castro et al., 12th Mechanical Engineering Design of Synchrotron Radiation Equipment and Instrumentation. JACOW Publishing (2023)
4. X. Wang et al., J. Synchrotron Radiat. **15**, 4 (2008)
5. S. Sharma, C. Spataro, *Proceedings of Mechanical Engineering Design of Synchrotron Radiation Equipment and Instrumentation* (JACOW Publishing, 2020)
6. Z. Liu et al., 11th Mechanical Engineering Design of Synchrotron Radiation Equipment and Instrumentation (MEDSI'20). JACOW Publishing (2020).
7. F. Rodrigues et al., Synchrotron Radiat. News. **32**, 5 (2019)
8. S. Zelenika et al., Nucl. Instrum. Methods Phys. Res. A. **467**, 99–102 (2001)
9. I.P. Martin et al., Proc. EPAC 2006. JACOW Publishing (2006)
10. Tseng, Tse-Chuan, et al., 6th Int. Particle Accelerator Conf. (IPAC'15). JACOW Publishing (2015).
11. F. Cianciosi et al., Proceedings, 9th Mechanical Engineering Design of Synchrotron Radiation Equipment and Instrumentation Conference. JACOW Publishing (2017)
12. J Seok, Low Emittance Rings Workshop 2024. CERN (2024)
13. S.J.S. Tabatabaei, A.M. Fattahi, Mech. Based Des. Struct. Mach. **50**, 4 (2022)